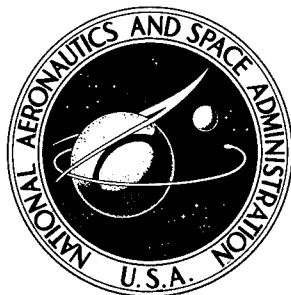


NASA TECHNICAL NOTE



NASA TN D-5453

NASA TN D-5453

DISTRIBUTION STATEMENT A
Approved for public release
Distribution Unlimited

STRESS CONCENTRATION AROUND BROKEN FILAMENTS IN A FILAMENT-STIFFENED SHEET

by *W. B. Fichter*

19960326 094

Langley Research Center

Langley Station, Hampton, Va.

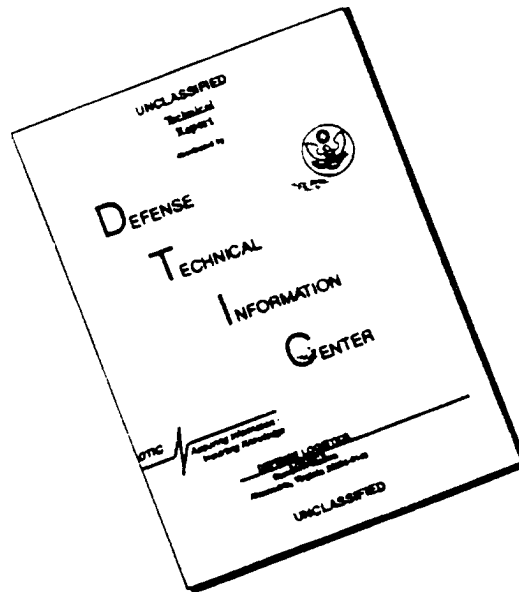
DTIC QUALITY INSPECTED 1

NATIONAL AERONAUTICS AND SPACE ADMINISTRATION • WASHINGTON, D. C. • OCTOBER 1969

DEPARTMENT OF DEFENSE
PLASTICS TECHNICAL EVALUATION CENTER
PICATINNY ARSENAL, DOVER, N. J.

PLASTEG 13057

DISCLAIMER NOTICE



THIS DOCUMENT IS BEST QUALITY AVAILABLE. THE COPY FURNISHED TO DTIC CONTAINED A SIGNIFICANT NUMBER OF PAGES WHICH DO NOT REPRODUCE LEGIBLY.

1. Report No. NASA TN D-5453	2. Government Accession No.	3. Recipient's Catalog No.	
4. Title and Subtitle STRESS CONCENTRATION AROUND BROKEN FILAMENTS IN A FILAMENT-STIFFENED SHEET		5. Report Date October 1969	6. Performing Organization Code
		8. Performing Organization Report No. L-5973	10. Work Unit No. 124-08-10-02-23
7. Author(s) W. B. Fichter	9. Performing Organization Name and Address NASA Langley Research Center Hampton, Va. 23365		11. Contract or Grant No.
12. Sponsoring Agency Name and Address National Aeronautics and Space Administration Washington, D.C. 20546			13. Type of Report and Period Covered Technical Note
		14. Sponsoring Agency Code	
15. Supplementary Notes This paper is based on part of a thesis entitled "Stress Concentrations in Filament-Stiffened Sheets" submitted in partial fulfillment of the requirements for the degree of Doctor of Philosophy in Engineering Mechanics, North Carolina State University, August 1969.			
16. Abstract <p>Stress distributions around single and double cuts (groups of adjacent broken filaments) in an idealized composite sheet consisting of parallel tension-carrying filaments embedded in a shear-carrying matrix are analyzed by an influence-function technique. Static-load concentration factors for two equal collinear cuts are obtained and are compared with some related results for a single cut. Dynamic-load concentration factors, corresponding to sudden breaking of filaments, also are obtained for two of the simplest double-cut cases. In addition, matrix shear forces are investigated for some single-cut and double-cut cases. Finally, loads in broken filaments are calculated for some single-cut cases, and their implications in some current failure analyses of composite materials are briefly discussed. The interaction between two collinear cuts is essentially local and is roughly confined to separation distances on the order of the cut length. For closely spaced cuts, however, the interaction between cuts is seen to be pronounced. For a single cut, an expression analogous to the filament load concentration factor is obtained for the maximum shear force in the matrix as a function of the cut length. The results suggest that for some combinations of constituent mechanical properties, the composite might be more susceptible to filament tensile failure at some cut lengths, but more susceptible to matrix shear failure at others.</p>			
17. Key Words Suggested by Author(s) Stress concentration Filament stiffened sheets Composite materials		18. Distribution Statement Unclassified - Unlimited	
19. Security Classif. (of this report) Unclassified	20. Security Classif. (of this page) Unclassified	21. No. of Pages 32	22. Price* \$3.00

STRESS CONCENTRATION AROUND BROKEN FILAMENTS
IN A FILAMENT-STIFFENED SHEET *

By W. B. Fichter
Langley Research Center

SUMMARY

Stress distributions around single and double cuts (groups of adjacent broken filaments) in an idealized composite sheet consisting of parallel tension-carrying filaments embedded in a shear-carrying matrix are analyzed by an influence-function technique. Static-load concentration factors for two equal collinear cuts are obtained and are compared with some related results for a single cut. Dynamic-load concentration factors, corresponding to sudden breaking of filaments, also are obtained for two of the simplest double-cut cases. In addition, matrix shear forces are investigated for some single-cut and double-cut cases. Finally, loads in broken filaments are calculated for some single-cut cases, and their implications in some current failure analyses of composite materials are briefly discussed.

The interaction between two collinear cuts is essentially local and is roughly confined to separation distances on the order of the cut length. For closely spaced cuts, however, the interaction between cuts is seen to be pronounced. For a single cut, an expression analogous to the filament load concentration factor is obtained for the maximum shear force in the matrix as a function of the cut length. The results suggest that for some combinations of constituent mechanical properties, the composite might be more susceptible to filament tensile failure at some cut lengths, but more susceptible to matrix shear failure at others.

INTRODUCTION

Much effort is currently being directed toward the development of lightweight composite materials typically composed of plastics and metals in which are embedded high-strength fibers. An extensive survey of composite materials research is contained in

*This paper is based on part of a thesis entitled "Stress Concentrations in Filament-Stiffened Sheets" submitted in partial fulfillment of the requirements for the degree of Doctor of Philosophy in Engineering Mechanics, North Carolina State University, August 1969.

reference 1. In studies of the tensile strength of fibrous composites (for example, refs. 1 and 2), it has been observed that failure can be initiated by local cuts or breaks in the filaments. A theory for predicting composite tensile strength which recognizes the statistical nature of filament strength as well as local cut distribution has been developed in reference 2. In the statistical approach, however, the stress concentration effects of flaw size and flaw distribution are generally ignored or treated rather approximately. Therefore, an analysis in which stress concentration effects are taken into account in more detail is desirable, and the present paper is directed toward determining some of these effects.

Analytical investigations of the stress fields around some isolated "cutouts" in an infinite flat sheet of parallel tension-carrying filaments embedded in a shear-carrying matrix are contained in reference 3. Included in these investigations is an analysis which yields the filament load concentration factor for a single straight cut across an arbitrary number of adjacent filaments (or, equivalently, a group of adjacent broken filaments). More recently, this analysis has been extended in reference 4 to problems of load concentration in composites with two-dimensional arrays of parallel filaments. Another logical extension of the analysis is to the problem of two cuts in the same filamentary sheet, since neighboring flaws in a filamentary composite can be expected to influence one another.

In the present paper an analysis is given of the stresses in a filament sheet weakened by two collinear cuts of arbitrary length. For the particular case of cuts of equal length, filament load concentration factors are computed for various combinations of cut length and distance between cuts. In addition, matrix shear forces and filament tensile forces are computed for several cases involving single and double cuts. For the case of a single cut, an expression analogous to the filament load concentration factor is obtained for the maximum matrix shear force as a function of cut length. Finally, the recovery of load by broken filaments is investigated for an idealized model and the results, as they pertain to statistical strength predictions such as those of reference 2, are briefly discussed.

SYMBOLS

d	filament center-line spacing
d_f	filament diameter
EA	extensional stiffness of a filament
E_n	Weber function

G	matrix shear modulus
h	effective thickness of matrix
I_n	modified Bessel function of first kind
J_n	Bessel function of first kind
$i, k, m, n, \left. \begin{array}{l} q, r, s \end{array} \right\}$	integers
K	filament load concentration factor
L_n	modified Struve function
M	mass per unit length associated with a filament
N_n	load in nth filament for influence-function solution (L_n of ref. 3)
P_n	dimensionless load in nth filament, p_n/p
p	force applied to each filament at infinity
p_n	load in nth filament
S_{max}	maximum dimensionless matrix shear force
S_n	dimensionless matrix shear force per unit length between nth and (n + 1)th filaments, $\frac{S_n}{p} \sqrt{\frac{EAd}{Gh}}$
s_n	matrix shear force per unit length between nth and (n + 1)th filaments
t	time
U_n	dimensionless displacement of nth filament, $\frac{u_n}{p} \sqrt{\frac{EAGh}{d}}$
u_n	displacement of nth filament

V_n	displacement of nth filament for influence-function solution
x	coordinate parallel to filaments
Γ	gamma function
ξ	dimensionless coordinate parallel to filaments, $x \sqrt{\frac{Gh}{EAd}}$
τ	dimensionless time, $t \sqrt{\frac{Gh}{Md}}$
θ	variable of integration

GOVERNING EQUATIONS

Insofar as is practical, the notation employed in reference 3 is retained in the present analysis. The model is shown in figure 1(a), along with the coordinate system and some notation. The analytical model is one commonly used in "shear lag" analyses, which does not account for local stress variations near the filament-matrix interface. It is composed of parallel tension-carrying members (filaments) embedded in a matrix which carries only shear. The filaments are separated by a constant distance d and are numbered from $-\infty$ to ∞ . The coordinate along the filaments is x and the displacement of the nth filament at location x is $u_n(x)$. The force in the nth filament, taken positive in tension, is denoted by $p_n(x)$ and is given in terms of u_n by

$$p_n(x) = EA \frac{du_n}{dx} \quad (1)$$

where EA is the extensional stiffness of the filament. The shear force per unit length between the nth and $(n + 1)$ th filaments is defined here by $s_n = \frac{Gh}{d}(u_{n+1} - u_n)$. Static equilibrium of an element of the nth filament then requires

$$\frac{d}{dx} p_n(x) + s_n(x) - s_{n-1}(x) = 0$$

or, in terms of displacements,

$$EA \frac{d^2 u_n}{dx^2} + \frac{Gh}{d}(u_{n+1} - 2u_n + u_{n-1}) = 0 \quad (2)$$

In figure 1(a), filaments -2, -1, 2, and 3 are shown cut at $x = 0$ for illustrative purposes. In general, for two collinear cuts through q and s filaments, let

$-(k + q) \leq n \leq -(k + 1)$ and $r + 1 \leq n \leq r + s$, respectively, denote the broken filaments, the two cuts being separated by $r + k + 1$ intact filaments. (See fig. 1(b).) Then the boundary conditions at $x = 0$ are

$$\left. \begin{aligned} u_n(0) = 0 & \quad (-k \leq n \leq r; -(k + q + 1) \leq n; n \geq r + s + 1) \\ p_n(0) = 0 & \quad (-(k + q) \leq n \leq -(k + 1); r + 1 \leq n \leq r + s) \end{aligned} \right\} \quad (3)$$

For x large, the force in each filament approaches the uniform applied force, denoted by p ; that is,

$$p_n(\pm\infty) = p \quad (4)$$

For convenience, let

$$\left. \begin{aligned} p_n &= pP_n \\ u_n &= p\sqrt{\frac{d}{EAGh}} U_n \\ s_n &= p\sqrt{\frac{Gh}{EAd}} S_n \\ x &= \sqrt{\frac{EAd}{Gh}} \xi \end{aligned} \right\} \quad (5)$$

Then the equilibrium equations and boundary conditions become

$$\frac{d^2 U_n}{d\xi^2} + U_{n+1} - 2U_n + U_{n-1} = 0 \quad (6)$$

$$\left. \begin{aligned} U_n(0) = 0 & \quad (n \leq -(k + q + 1); -k \leq n \leq r; n \geq r + s + 1) \\ P_n(0) = 0 & \quad (-(k + q) \leq n \leq -(k + 1); r + 1 \leq n \leq r + s) \\ P_n(\pm\infty) = 1 & \end{aligned} \right\} \quad (7)$$

The dimensionless forces and displacements are related by

$$\left. \begin{aligned} P_n &= \frac{dU_n}{d\xi} \\ S_n &= U_{n+1} - U_n \end{aligned} \right\} \quad (8)$$

SOLUTIONS

The mixed boundary value problem defined by equations (6), (7), and (8) can be solved by use of the influence-function technique employed in reference 3 to solve the single-cut problem. The influence functions $V_n(\xi)$ and $N_n(\xi) = \frac{dV_n}{d\xi}(\xi)$ are, respectively, the non-dimensional displacement and force in the n th filament when the filament sheet is completely cut along $\xi = 0$ and the zeroth filament is displaced a unit amount at $\xi = 0$ while all other filaments are held fixed at $\xi = 0$. In terms of $V_n(\xi)$ and $N_n(\xi)$ ($L_n(\xi)$ in ref. 3), the dimensionless force and displacement in the n th filament are given by

$$\left. \begin{aligned} P_n(\xi) &= 1 + \sum_{i=-\infty}^{\infty} N_{n-i}(\xi) U_i(0) \\ U_n(\xi) &= \xi + \sum_{i=-\infty}^{\infty} V_{n-i}(\xi) U_i(0) \end{aligned} \right\} \quad (9)$$

In reference 3, $V_n(\xi)$ has been found to be

$$V_n(\xi) = \frac{1}{\pi} \int_0^\pi \cos n\theta e^{-2\xi \sin \frac{\theta}{2}} d\theta \quad (10)$$

Application of boundary conditions (7) to equations (9) yields

$$\left. \begin{aligned} P_n(\xi) &= 1 + \sum_{i=-(k+q)}^{-(k+1)} N_{n-i}(\xi) U_i(0) + \sum_{i=r+1}^{r+s} N_{n-i}(\xi) U_i(0) \\ U_n(\xi) &= \xi + \sum_{i=-(k+q)}^{-(k+1)} V_{n-i}(\xi) U_i(0) + \sum_{i=r+1}^{r+s} V_{n-i}(\xi) U_i(0) \end{aligned} \right\} \quad (11)$$

since $U_i(0) = 0$ for other values of i , and

$$0 = 1 + \sum_{i=-(k+q)}^{-(k+1)} N_{n-i}(0) U_i(0) + \sum_{i=r+1}^{r+s} N_{n-i}(0) U_i(0) \quad (12)$$

$(-(k+q) \leq n \leq -(k+1); r+1 \leq n \leq r+s)$

which expresses the condition of zero load on the ends of the broken filaments. Equations (12) constitute a set of $q + s$ linear algebraic equations in the $q + s$ unknowns $U_n(0)$. Their solution set can be substituted into equations (11) to obtain expressions for load and displacement in any filament.

However, before the loads and displacements can be calculated, the integral representation of the influence functions $V_n(\xi)$ and $N_n(\xi)$ must be evaluated. Only $N_n(0) = \frac{dV_n}{d\xi}(0)$ has been evaluated in reference 3 because the computation of load concentration factors, which was the main purpose of that investigation, does not require the evaluation of the influence functions for nonzero values of ξ . Equation (10) can also be written as

$$V_n(\xi) = \frac{1}{\pi} \int_0^\pi \cos 2n\theta e^{-2\xi \sin \theta} d\theta \quad (13)$$

Integration of this expression gives

$$V_n(\xi) = J_{2n}(2i\xi) - iE_{2n}(2i\xi)$$

where i denotes $\sqrt{-1}$, J_{2n} is the Bessel function of the first kind of order $2n$, and E_{2n} is the Weber function of order $2n$. (See ref. 5.) In terms of functions with real arguments,

$$V_n(\xi) = (-1)^n \left[I_{2n}(2\xi) - L_{2n}(2\xi) - \frac{1}{\pi} \sum_{k=0}^{n-1} (-1)^k \frac{\Gamma(k + \frac{1}{2}) \xi^{2n-2k-1}}{\Gamma(2n + \frac{1}{2} - k)} \right] \quad (n \geq 0) \quad (14)$$

in which I_{2n} is the modified Bessel function of the first kind, L_{2n} is the modified Struve function (see ref. 5), and the finite sum must be taken to be zero for $n = 0$. A similar expression for $V_n(\xi)$ can be derived for $n < 0$; however, it is obvious from equation (13) that $V_{-n}(\xi) = V_n(\xi)$. Differentiation of equation (14) yields

$$N_n(\xi) = (-1)^n \left\{ I_{2n+1}(2\xi) + I_{2n-1}(2\xi) - \left[L_{2n+1}(2\xi) + L_{2n-1}(2\xi) + \frac{\xi^{2n}}{\pi^{1/2} \Gamma(2n + \frac{3}{2})} \right] - \frac{1}{\pi} \sum_{k=0}^{n-1} (-1)^k \frac{(2n - 2k - 1) \Gamma(k + \frac{1}{2}) \xi^{2n-2k-2}}{\Gamma(2n + \frac{1}{2} - k)} \right\} \quad (n \geq 0) \quad (15)$$

in which the finite sum again is to be omitted for $n = 0$. From equation (15) it is found that

$$N_n(0) = \frac{4}{\pi(4n^2 - 1)} \quad (16)$$

which is in agreement with reference 3.

With substitution of the appropriate values from equation (16), equations (12), which are merely linear algebraic equations, can be solved for the displacements of the ends of the broken filaments $U_n(0)$. Then the solutions to equations (12), along with the influence functions given by equations (14) and (15), can be substituted into equations (11) to obtain the load and displacement at any point in the filamentary sheet. However, because each cut may traverse any number of filaments and the two cuts may be separated by any number of intact filaments, the general case of two collinear cuts is without symmetry. Hence, calculations covering reasonably wide variations of the pertinent parameters would entail considerable computational effort. If the problem is simplified, however, by requiring the cuts to be of equal length, the most essential features of the two-cut problem are retained and the computational effort is greatly reduced through consideration of the resulting symmetries.

In what follows, then, it is assumed that the two collinear cuts are of equal length. In the analysis of this reduced problem, one of two cases arises, depending upon whether the number of filaments between the cuts (henceforth called "interior filaments") is even or odd. The analysis of these two cases is presented in the appendix, pertinent results being drawn from there as appropriate.

Filament Loads

In the case of a single cut across n consecutive filaments (beginning with the zeroth filament), the load and displacement in the r th filament were found in reference 3 to be

$$P_r(\xi) = 1 + \sum_{i=0}^{n-1} N_{r-i}(\xi) U_i(0) \quad (17)$$

and

$$U_r(\xi) = \xi + \sum_{i=0}^{n-1} V_{r-i}(\xi) U_i(0) \quad (18)$$

where the $U_i(0)$ terms are the solutions to the n simultaneous equations

$$0 = 1 + \sum_{i=0}^{n-1} N_{r-i}(0) U_i(0) \quad (0 \leq r \leq n - 1) \quad (19)$$

For the case of two equal-length collinear cuts separated by any number of intact filaments, expressions for the load and displacement in any filament are derived in the appendix.

In reference 3 the load concentration factor for a single cut across n filaments was found to be

$$K_n = P_n(0) = 1 + \sum_{i=0}^{n-1} N_{n-i}(0) U_i(0) \quad (20)$$

which is the maximum load in the filament just ahead of the cut. For double cuts, the most highly stressed filaments are the outermost of the filaments between the cuts and, again, their maximum load occurs at $\xi = 0$. In the appendix, expressions for the load concentration factors have been found for cases involving odd and even numbers of interior filaments. For an odd number $2r + 1$ of intact filaments between two cuts, each across n filaments, the load concentration factor is

$$K_{n,2r+1} = 1 + \sum_{i=r+1}^{r+n} [N_{r+i}(0) + N_{r-i}(0)] U_i(0) \quad (21)$$

where the $U_i(0)$ terms are the solutions to equations (A4) for a specific value of n ; and for an even number $2r$ of interior filaments,

$$K_{n,2r} = 1 + \sum_{i=r}^{r+n-1} [N_{r+i}(0) + N_{r-i-1}(0)] U_i(0) \quad (22)$$

where the $U_i(0)$ terms are calculated from equations (A10).

Shear Loads

The dimensionless shear force per unit length between the n th and $(n + 1)^{\text{th}}$ filaments is given by

$$S_n(\xi) = U_{n+1}(\xi) - U_n(\xi) \quad (23)$$

In either a single-cut or double-cut configuration, the greatest matrix shear force is between a broken filament and an unbroken one. In the case of a double cut, the unbroken filament is an interior one.

To find the matrix shear forces in a single-cut problem, the solutions to the boundary load conditions (19) are substituted into equation (18) to obtain displacements, and those results are used in equation (23). In a double-cut problem, either equations (A4) or (A10)

are solved, depending on the number of interior filaments, and the solutions are substituted into the second of either equation (A3) or (A9), respectively, and then equation (23) is used.

Calculations of matrix shear forces have been made for some single-cut and double-cut cases. The calculations are restricted in each case to the matrix area between two filaments which experiences the greatest shear stress. The solutions are:

For single cut across one filament:

$$S_0(\xi) = \frac{\pi}{4} \left\{ \frac{2}{\pi\xi} - 2 \left[\bar{I}_0(2\xi) - L_0(2\xi) \right] - \frac{1}{\xi} \left[\bar{L}_{-1}(2\xi) - I_1(2\xi) \right] \right\} \quad (24)$$

where

$$S_0(0) = -\frac{\pi}{4}$$

For single cut across two filaments:

$$S_1(\xi) = \frac{3\pi}{8} \left\{ \frac{6}{\xi^2} \left[\bar{I}_0(2\xi) - L_0(2\xi) \right] + \frac{2}{\xi} \left(2 + \frac{3}{\xi^2} \right) \left[\bar{L}_{-1}(2\xi) - I_1(2\xi) \right] - \frac{12}{\pi\xi^3} \right\} \quad (25)$$

where

$$S_1(0) = -\frac{3\pi}{8}$$

For single cut across three filaments:

$$S_2(\xi) = -\frac{3\pi}{16} \left\{ \left(4 + \frac{87}{\xi^2} + \frac{300}{\xi^4} \right) \left[\bar{I}_0(2\xi) - L_0(2\xi) \right] + \frac{1}{\xi} \left(20 + \frac{237}{\xi^2} \right) \right. \\ \left. + \frac{300}{\xi^4} \left[\bar{L}_{-1}(2\xi) - I_1(2\xi) \right] - \frac{4}{\pi\xi} - \frac{74}{\pi\xi^3} - \frac{600}{\pi\xi^5} \right\} \quad (26)$$

where

$$S_2(0) = -\frac{15\pi}{32}$$

For two cuts, each across one filament, with one interior filament:

$$\bar{S}_0(\xi) = \frac{15\pi}{56} \left\{ 2 \left(2 + \frac{3}{\xi^2} \right) \left[\bar{I}_0(2\xi) - L_0(2\xi) \right] + \frac{6}{\xi} \left(1 + \frac{1}{\xi^2} \right) \left[\bar{L}_{-1}(2\xi) - I_1(2\xi) \right] - \frac{4}{\pi\xi} - \frac{12}{\pi\xi^3} \right\} \quad (27)$$

where

$$\bar{S}_0(0) = \frac{15\pi}{56}$$

For two cuts, each across two filaments, with one interior filament:

$$\begin{aligned} \bar{S}_0(\xi) = & \frac{5565\pi}{2(6512)} \left(2 \left(2 + \frac{3}{\xi^2} \right) [\bar{I}_0(2\xi) - L_0(2\xi)] + \frac{6}{\xi} \left(1 + \frac{1}{\xi^2} \right) [\bar{L}_{-1}(2\xi) - I_1(2\xi)] \right. \\ & - \frac{4}{\pi\xi} - \frac{12}{\pi\xi^3} - \frac{51}{53} \left. \left(4 \left(1 + \frac{12}{\xi^2} + \frac{30}{\xi^4} \right) [\bar{I}_0(2\xi) - L_0(2\xi)] \right. \right. \\ & \left. \left. + \frac{6}{\xi} \left(3 + \frac{18}{\xi^2} + \frac{20}{\xi^4} \right) [\bar{L}_{-1}(2\xi) - I_1(2\xi)] - \frac{4}{\pi\xi} - \frac{56}{\pi\xi^3} - \frac{240}{\pi\xi^5} \right) \right) \end{aligned} \quad (28)$$

where

$$\bar{S}_0(0) = \frac{5565\pi}{2(6512)}$$

and where the bars are used to identify double-cut shear forces. A comparison of equations (27) and (28) will indicate how rapidly the complexity of double-cut shear force calculations grows with cut length.

RESULTS AND DISCUSSION

The solutions presented in the preceding section have been employed to investigate various phenomena associated with the breaking of filaments, such as static and dynamic load concentration in filaments, matrix shear force growth with cut length, as well as decay of matrix shear force and recovery of load by broken filaments as functions of axial distance from the cut.

Load Concentration Factors

Tensile loads.- In reference 3 the static load concentration factor for a single cut across n consecutive filaments was found to be

$$K_n = \frac{4 \cdot 6 \cdot 8 \cdots (2n + 2)}{3 \cdot 5 \cdot 7 \cdots (2n + 1)} \quad (n = 1, 2, 3, \dots) \quad (29)$$

In the present paper, filament load concentration factors for two collinear cuts $K_{n,m}$ each across n filaments, separated by m intact filaments, have been calculated for n from 1 to 8 and m from 1 to 16. The results are presented in table I and are plotted in figure 2, along with the single-cut factor K_n for purposes of comparison. It might be noted here that K_n is the asymptotic value of $K_{n,m}$ for large m , that is, for large distances between the cuts. It can be seen in figure 2 that the interaction between collinear cuts is essentially local, being confined to separation distances which are on the order

of the cut length. For cuts which are farther apart, the results do not differ conspicuously from their asymptotic, single-cut values. Thus, when two cuts are separated by distances which are greater than their lengths, each cut can be considered independently with little loss of accuracy.

The values of $K_{n,m}$ for closely spaced cuts, however, increase rapidly when m becomes small. Hence, $K_{n,m}$ for m small is of particular interest, since it is associated with states of severe load concentration. In order to examine the relative severity of double cuts and comparable single cuts, double-cut factors for closely spaced cuts are plotted in figure 3 along with factors for single cuts of comparable total length. In terms of the notation employed here, $K_{n,1}$ and $K_{n,2}$ are compared with single-cut factors denoted by K_{2n} , K_{2n+1} , and K_{2n+2} . These particular values of the single-cut factor are employed because they represent either the same total number $2n$ of broken filaments or the number $2n + 1$ or $2n + 2$ which would be broken if the double cuts separated by one or two intact filaments, characterized by $K_{n,1}$ or $K_{n,2}$, were to coalesce.

It can be seen in figure 3 that the load concentration factors for the double cut with one interior filament $K_{n,1}$ is greater than those for a single cut across an equal number of filaments when more than two filaments are broken. Also, the factors for the double cut with two interior filaments $K_{n,2}$ are greater than those for a single cut across an equal number of filaments when 15 or more filaments are broken. Thus, it appears that the longest cut does not necessarily induce the most severe stress state.

This result suggests that a composite structural design criterion based on residual strength of the composite in the presence of a single cut of prescribed length could be unconservative, even though only cuts of lesser length were present.

In reference 3 dynamic load concentration factors were obtained for cases in which a single cut is suddenly introduced in a stretched filament sheet and, in a separate analysis, an apparent upper limit of 1.27 was found for the dynamic overshoot (ratio of maximum dynamic and static load concentration factors). To investigate the possibility of a departure from the trend for a single cut, dynamic load concentration factors have been computed for two of the simplest double cut cases. The dynamic analysis was carried out by inserting the appropriate inertia term in equation (2) and utilizing the Laplace transform theory in the manner of reference 3. The results are presented in figure 4, where some single cut results are reproduced for purposes of comparison. For the two double-cut cases, in which totals of two and four filaments were suddenly broken, one remaining intact between them, the dynamic overshoots were found to be 1.22 and 1.23, respectively, and are in the range of previously obtained single-cut results. The fact that additional double-cut calculations have not been made because of their rapidly increasing complexity precludes the drawing of sweeping conclusions concerning the

overall behavior of the double-cut dynamic overshoot; however, the present limited calculations suggest that departure from the range of single-cut values is unlikely.

Shear loads.- Although the present composite model accounts for matrix shear stress in only an approximate manner, it is believed that matrix shear-force calculations are of at least qualitative interest. A result which was not obtained in reference 3, but which can be extracted from the analysis presented there, is the magnitude of the most severe shear force at a single cut as a function of the number of cut filaments, which might be thought of as a shear-force concentration factor S_{\max} . For a cut which starts at the zeroth filament and severs n filaments, the most severe shear force is given by

$$S_{\max} = |S_n(0)| = U_0(0) \quad (30)$$

where S_{\max} is defined as the absolute value of the peak shear force, and where $U_0(0)$ is the nondimensional displacement of the end of the zeroth filament, which varies with the number of cut filaments. Solution of equations (19), (18), and (23) for the first six values of n yields the following values of S_{\max} (see also eqs. (24), (25), and (26)):

n	S_{\max}
1	0.785
2	1.178
3	1.473
4	1.718
5	1.933
6	2.126

Inspection of these values in fractional form indicated that they conformed to the expression

$$\frac{4}{\pi} S_{\max} = \frac{(2n - 1)!}{2^{2n-2} [(n - 1)!]^2} \quad (31)$$

By using equations (27) and (28), a few results were also obtained for the shear load concentration factor \bar{S}_{\max} for the two simplest double-cut configurations in which a single intact filament separates the cuts. Solutions for 2 and 4 broken filaments yield

n	\bar{S}_{\max}
2	0.841
4	1.342

Unlike tensile load concentration factors for closely spaced cuts, these limited results suggest that the shear load concentration factors for double cuts are less than those for single cuts with the same number of cut filaments.

A further consideration in comparing shear and tensile load concentration factors is their relative rates of increase with increasing number of cut filaments. In figure 5, the shear concentration factor S_{\max} for single cuts is compared with the tensile load concentration factor K_n for values of n up to 13. The shear force can be seen to increase more rapidly than the tensile force, particularly for small values of n . Both K_n and S_{\max} are unbounded as n approaches infinity. However, their relative magnitudes for large n can be determined by writing equation (29) in the form

$$K_n = \frac{2^{2n} n! (n+1)!}{(2n+1)!}$$

and forming the ratio

$$\frac{\frac{4}{\pi} S_{\max}}{K_n} = \frac{n(2n+1)[(2n)!]^2}{2^{4n-1}(n+1)(n!)^4} \quad (32)$$

By the use of asymptotic formulas for the factorial function, it is found that

$$\frac{S_{\max}}{K_n} \rightarrow 1 \quad (n \rightarrow \infty) \quad (33)$$

Equations (32) and (33) indicate that the maximum dimensionless matrix shear force and filament tensile force are of comparable magnitude for all values of n . They are approximately equal for large values of n , although, as noted, the maximum shear force initially increases more rapidly than the tensile force. This difference in slopes for small n suggests that some composite materials could be more susceptible to tensile failure of the filaments when only small flaws are present, but might be more susceptible to matrix shear failure when weakened by larger flaws.

The longitudinal variation of the shear loads was also investigated. In figure 6, the most severe matrix shear forces for single cuts across one, two, and three filaments (see eqs. (24), (25), and (26)) are plotted as functions of the axial distance from the cut. Also shown are results for the two simplest double-cut configurations (see eqs. (27) and (28)) in which a single intact filament separates the cuts. The curves are normalized with respect to their peak values, which can be obtained from the table of amplitudes in figure 6 along with the pertinent equation from equations (5). It can be seen that the peak values increase with cut length. The normalized curves differ from one another in their rates of decay with axial distance from the cut, the decay generally being slower for longer cuts. It might also be noted that the double-cut shear loads decay somewhat more rapidly than those for the single cuts.

Loads in Broken Filaments

For a single cut across n consecutive filaments (starting with the zeroth filament), the load in the i th filament is given by

$$P_i(\xi) = 1 + \sum_{k=0}^{n-1} N_{i-k}(\xi) U_k(0)$$

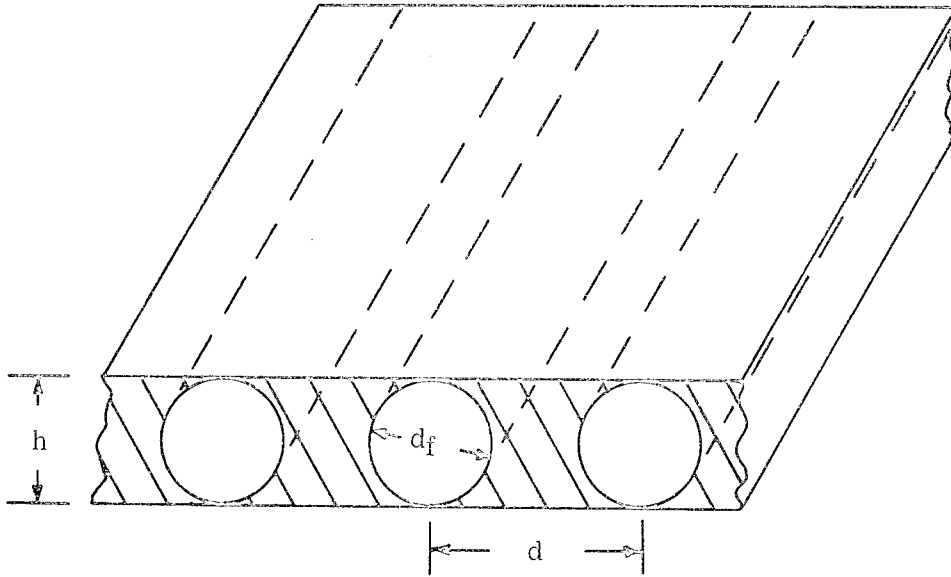
where the n broken filaments are identified by $i = 0, 1, \dots, n - 1$, and each $U_k(0)$ is one of a unique set associated with a specific value of n . The $U_k(0)$ values are obtained by solution of equations (19).

Loads in the broken filaments have been calculated for a single cut across one, two, and three filaments. The results are plotted in figure 7, where it can be seen that the length over which a broken filament carries less than a particular fraction of its load can vary considerably with the number of broken filaments. The 90-percent load-recovery line has been added for later reference. With slightly more labor, similar results can be obtained for various double-cut configurations; however, results for double cuts are not expected to exhibit significantly different trends. For this reason, and because illustration of the effect of cut length on filament load recovery is the main purpose of the calculations, loads in broken filaments have not been calculated for double cuts.

Ineffective Length Calculation

In reference 2, the ineffective length of a filament is defined as that portion of a broken filament which supports less than 90 percent of the load applied at infinity. Studies cited in references 1 and 2 suggest that the ineffective length, based on a load-recovery fraction of 90 percent, of a single broken filament embedded in a matrix can range from less than one up to several hundred filament diameters, depending on the geometry and the mechanical properties of the constituents. Calculations have been made in reference 2, for example, of ineffective length as a function of filament volume fraction v_f , and E/G , the ratio of filament Young's modulus to matrix shear modulus. Results are presented in the form of a family of curves, each member of which corresponds to a particular filament volume fraction.

In the case of a composite containing a cut, an additional parameter which would be expected to influence the ineffective length is the number of broken filaments. With the aid of an idealized model, results from the present study can be used to obtain an indication of the influence of this parameter. A typical cross section of this model is shown in the sketch. For the present ineffective length calculations, it is assumed that the thickness of the sheet is equal to the filament diameter, and that in the matrix between any two adjacent filaments the shear stress is constant at a given axial location. Then for this



model the filament volume fraction is given by $v_f = \frac{\pi d_f^2}{4d}$ where d_f is the diameter of a filament and d is the filament spacing.

In terms of the pertinent mechanical and geometrical parameters, the axial distance along a filament is given by

$$x = \sqrt{\frac{EAd}{Gh}} \xi$$

which for the idealized model becomes

$$\frac{x}{d_f} = \frac{\pi}{4} \sqrt{\frac{E}{Gv_f}} \xi \quad (34)$$

In order to obtain estimates of ineffective length changes due to the breaking of additional filaments, it is necessary to determine from figure 7 the values of ξ , denoted by ξ' , at which the broken filaments of interest have recovered a stipulated fraction of their far-field load. These values of ξ , along with appropriate values of E/G and v_f , are then substituted into equation (34) to obtain values of the nondimensional ineffective length, denoted by x'/d_f .

This procedure has been carried out for two values of v_f and a range of values of E/G , the filament being considered ineffective wherever it supports less than 90 percent of its far-field load. The cases of cuts across one, two, and three adjacent filaments have been considered. The results are presented in figure 8. In the case of the cut across three filaments, the 90-percent recovery figure pertains to either of the two outer

filaments in the cut rather than to the middle filament which would have yielded even greater values of ineffective length.

The mathematical model employed in the analysis of reference 2 consists of a single filament encased in a thin layer of shear-carrying material (binder) which, in turn, is embedded in an infinite body to which are assigned the average stiffness properties of the composite material. Hence, interaction between neighboring filaments is ignored. In addition, shear stresses in the average material are assumed to decay in a negligible distance from its interface with the binder material. Because of these basic differences with the present model, the results of reference 2 are not plotted in figure 8. It should be noted, however, that the results of reference 2 yield a single curve for each filament volume fraction, whereas the present results yield a family of curves, each member of which corresponds to a particular number of broken filaments. In addition, the analysis of reference 2 predicts a more rapid recovery of load by broken filaments than does the present analysis. As can be seen in figure 8, large changes in filament ineffective length can result from varying the number of broken filaments. The results suggest that this effect should perhaps be accounted for in statistical studies of the strength of filamentary composites.

CONCLUDING REMARKS

An analysis has been made of the loads and deformations in a filament-stiffened sheet which has been weakened by two collinear cuts. Also, some results for the case of a single cut, in addition to those previously reported, have been obtained. It has been found that significant interaction between collinear cuts is largely restricted to cases in which the distance between cuts is no greater than the cut length. It is seen that two closely spaced cuts can cause greater stress concentration than a single cut across a comparable total number of filaments. Limited calculations of dynamic stress concentration factors for suddenly introduced collinear cuts support the earlier conclusion that dynamic effects are not of great importance in filamentary composites of the type investigated.

Calculations of loads in broken filaments show significant changes in ineffective filament length with cut length; thus, statistical strength analyses of composite materials should consider the incorporation of a flaw-size parameter.

Calculations for single cuts of various lengths show that maximum shear forces grow more rapidly with cut length than maximum tensile forces. Such calculations might be useful in determining whether a composite material is more susceptible to shear failure or tensile failure.

The present analysis is based on linear small-deflection theory of a single sheet, whereas filamentary composites usually are many filaments thick and are subject to various nonlinear effects such as plastic deformations, large deflections, and straightening of the filaments. Although these effects would be expected to exert some perturbing influence, the present results would be expected to remain qualitatively descriptive of load concentration effects in filamentary composites of the type investigated.

Langley Research Center,
National Aeronautics and Space Administration,
Langley Station, Hampton, Va., June 30, 1969.

APPENDIX

STRESS CONCENTRATION FACTORS FOR TWO EQUAL-LENGTH COLLINEAR CUTS

In this appendix attention is restricted to problems in which the two collinear cuts are of equal length. This restriction is effected by setting q equal to s in equations (11) and (12); this procedure yields

$$\left. \begin{aligned} P_n(\xi) &= 1 + \sum_{i=(k+s)}^{-(k+1)} N_{n-i}(\xi) U_i(0) + \sum_{i=r+1}^{r+s} N_{n-i}(\xi) U_i(0) \\ U_n(\xi) &= \xi + \sum_{i=-(k+s)}^{-(k+1)} V_{n-i}(\xi) U_i(0) + \sum_{i=r+1}^{r+s} V_{n-i}(\xi) U_i(0) \end{aligned} \right\} \quad (A1)$$

and

$$0 = 1 + \sum_{i=-(k+s)}^{-(k+1)} N_{n-i}(0) U_i(0) + \sum_{i=r+1}^{r+s} N_{n-i}(0) U_i(0) \quad (A2)$$

$(-(k+s) \leq n \leq -(k+1); r+1 \leq n \leq r+s)$

One of two cases arises, depending on whether the number of intact filaments between the cuts (interior filaments) is odd or even. The case of an odd number of interior filaments is treated first.

Odd Number of Interior Filaments

When the two cuts are of equal length, the displacements are symmetric with respect to the line which equally divides the group of interior filaments. In this case it is convenient to take the zeroth filament as the line of symmetry so that $k = r$ in equations (A1) and (A2) and the total number of interior filaments is $2r + 1$. With $U_i(0) = U_{-i}(0)$ because of symmetry, equations (A1) and (A2) become after some manipulation

APPENDIX

$$\left. \begin{aligned} P_n(\xi) &= 1 + \sum_{i=r+1}^{r+s} [N_{n+i}(\xi) + N_{n-i}(\xi)] U_i(0) \\ U_n(\xi) &= \xi + \sum_{i=r+1}^{r+s} [V_{n+i}(\xi) + V_{n-i}(\xi)] U_i(0) \end{aligned} \right\} \quad (A3)$$

and

$$0 = 1 + \sum_{i=r+1}^{r+s} [N_{n+i}(0) + N_{n-i}(0)] U_i(0) \quad (r+1 \leq n \leq r+s) \quad (A4)$$

The maximum load will occur adjacent to the cuts ($\xi = 0$) in the two outermost interior filaments ($n = \pm r$). Hence, from the first of equations (A3), the stress concentration factor for two cuts across s filaments separated by $2r + 1$ filaments is

$$K_{S,2r+1} = P_r(0) = 1 + \sum_{i=r+1}^{r+s} [N_{r+i}(0) + N_{r-i}(0)] U_i(0) \quad (A5)$$

where the $U_i(0)$ terms are calculated from equation (A4) for specified values of r and s .

Even Number of Interior Filaments

In this case, the interior filaments are assumed to be identified by $-k \leq n \leq r$, which with $r = k - 1$ becomes $-k \leq n \leq k - 1$. Equations (A1) and (A2) take the form

$$\left. \begin{aligned} P_n(\xi) &= 1 + \sum_{i=-(k+s)}^{-(k+1)} N_{n-i}(\xi) U_i(0) + \sum_{i=k}^{k+s-1} N_{n-i}(\xi) U_i(0) \\ U_n(\xi) &= \xi + \sum_{i=-(k+s)}^{-(k+1)} V_{n-i}(\xi) U_i(0) + \sum_{i=k}^{k+s-1} V_{n-i}(\xi) U_i(0) \end{aligned} \right\} \quad (A6)$$

and

APPENDIX

$$0 = 1 + \sum_{i=-(k+s)}^{-(k+1)} N_{n-i}(0) U_i(0) + \sum_{i=k}^{k+s-1} N_{n-i}(0) U_i(0) \quad (- (k + s) \leq n \leq - (k + 1); k \leq n \leq k + s - 1) \quad (A7)$$

For this configuration, the axial line of symmetry is located between the filaments numbered 0 and -1, which means that

$$U_{-i}(0) = U_{i-1}(0) \quad (A8)$$

After substitution from equation (A8) and some manipulation, equations (A6) and (A7) become

$$\left. \begin{aligned} P_n(\xi) &= 1 + \sum_{i=r}^{r+s-1} [N_{n+i+1}(\xi) + N_{n-i}(\xi)] U_i(0) \\ U_n(\xi) &= \xi + \sum_{i=r}^{r+s-1} [V_{n+i+1}(\xi) + V_{n-i}(\xi)] U_i(0) \end{aligned} \right\} \quad (A9)$$

and

$$0 = 1 + \sum_{i=r}^{r+s-1} [N_{n+i+1}(0) + N_{n-i}(0)] U_i(0) \quad (r \leq n \leq r + s - 1) \quad (A10)$$

In this case the maximum load occurs for $n = -r, r - 1$. Then with $n = r - 1$ in the first of equations (A9), the stress concentration factor for two cuts across s filaments, separated by $2r$ filaments, is

$$K_{S,2r} = P_{r-1}(0) = 1 + \sum_{i=r}^{r+s-1} [N_{r+i}(0) + N_{r-i-1}(0)] U_i(0) \quad (A11)$$

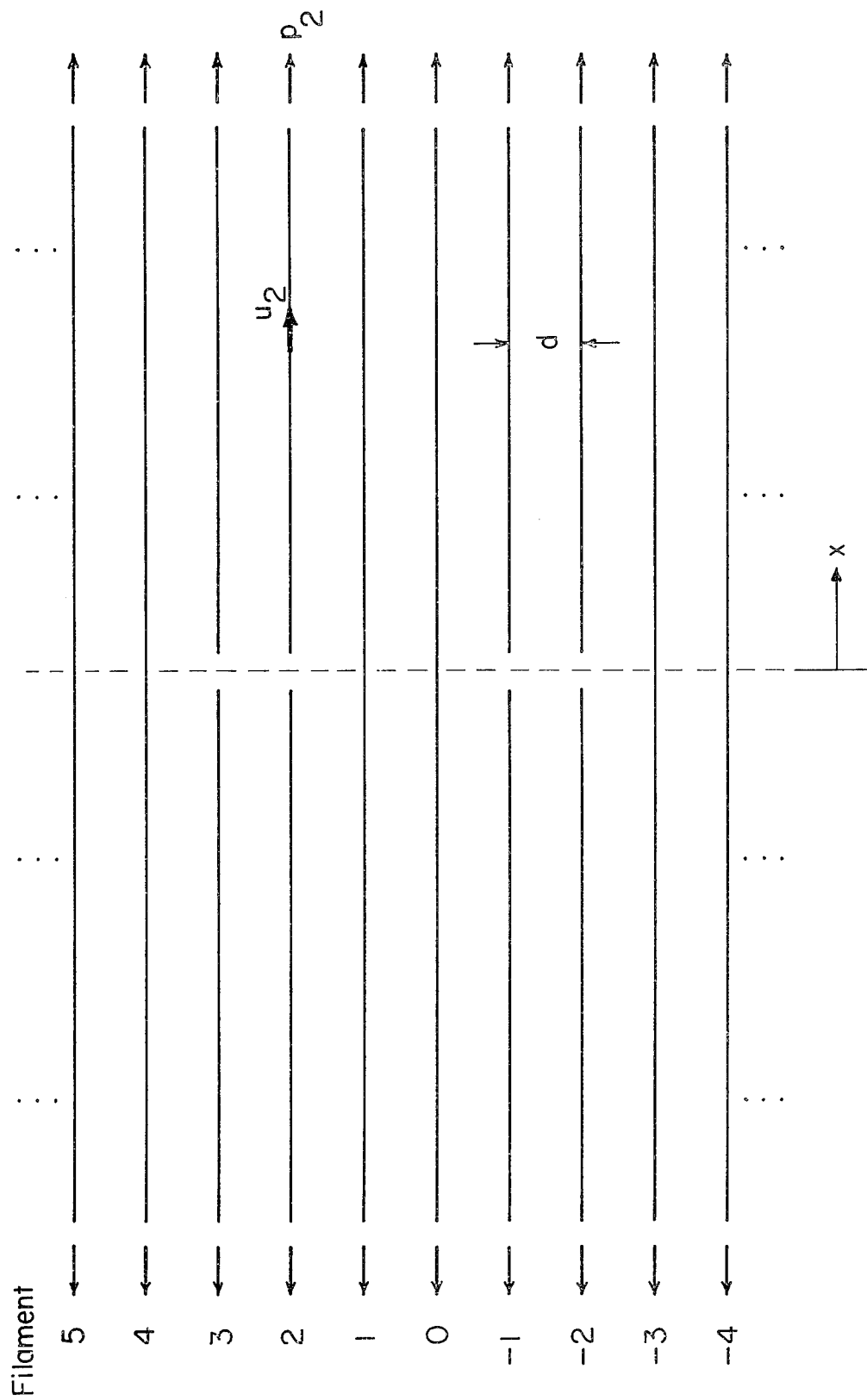
where the $U_i(0)$ terms are calculated from equations (A10) for specified values of r and s .

REFERENCES

1. Kelly, A.; and Davies, G. J.: The Principles of the Fibre Reinforcement of Metals. Met. Rev., vol. 10, no. 37, 1965, pp. 1-78.
2. Rosen, B. Walter: Mechanics of Composite Strengthening. Fiber Composite Materials, Amer. Soc. Metals, c.1965, pp. 37-75.
3. Hedgepeth, John M.: Stress Concentrations in Filamentary Structures. NASA TN D-882, 1961.
4. Hedgepeth, John M.; and Van Dyke, Peter: Local Stress Concentrations in Imperfect Filamentary Composite Materials. J. Compos. Mater., vol. 1, no. 3, July 1967, pp. 294-309.
5. Abramowitz, Milton; and Stegun, Irene A., eds.: Handbook of Mathematical Functions With Formulas, Graphs, and Mathematical Tables. Nat. Bur. Stand., Appl. Math. Ser. 55, U.S. Dep. Com., June 1964.

TABLE I.- LOAD CONCENTRATION FACTORS FOR TWO
COLLINEAR CUTS OF EQUAL LENGTH

Number of filaments between cuts	Load concentration factors when the number of filaments in each cut is -							
	1	2	3	4	5	6	7	8
1	1.714	2.359	2.964	3.543	4.102	4.646	5.177	5.698
2	1.412	1.788	2.142	2.481	2.808	3.126	3.436	3.740
3	1.368	1.690	1.989	2.272	2.543	2.805	3.061	3.310
4	1.353	1.654	1.928	2.185	2.430	2.666	2.895	3.118
5	1.346	1.636	1.897	2.140	2.370	2.590	2.803	3.009
6	1.342	1.626	1.879	2.113	2.333	2.542	2.745	2.940
7	1.340	1.620	1.867	2.095	2.308	2.510	2.705	2.893
8	1.338	1.615	1.859	2.082	2.290	2.488	2.677	2.859
9		1.612	1.854	2.073	2.278	2.471	2.655	2.833
10			1.849	2.066	2.268	2.458	2.639	2.813
11			1.846	2.061	2.261	2.448	2.626	2.798
12				2.057	2.255	2.440	2.616	2.785
13				2.054	2.250	2.434	2.608	2.775
14					2.246	2.428	2.601	2.766
15					2.243	2.424	2.595	2.759
16						2.420	2.590	2.753



(a) Double cuts across filaments -2, -1, 2, and 3.

Figure 1.- Coordinate and notation systems.

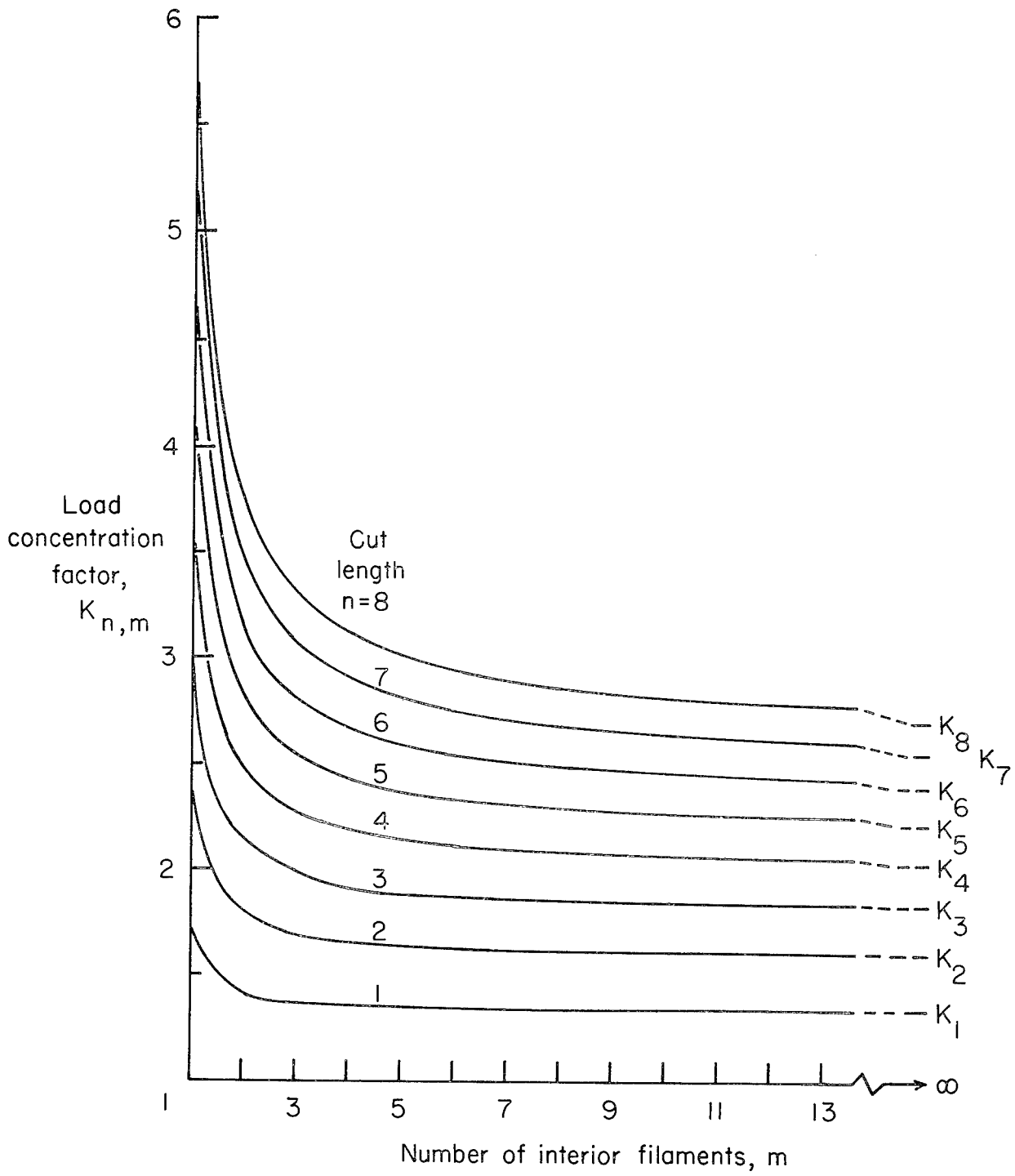


Figure 2.- Filament load concentration factors for equal-length collinear cuts.

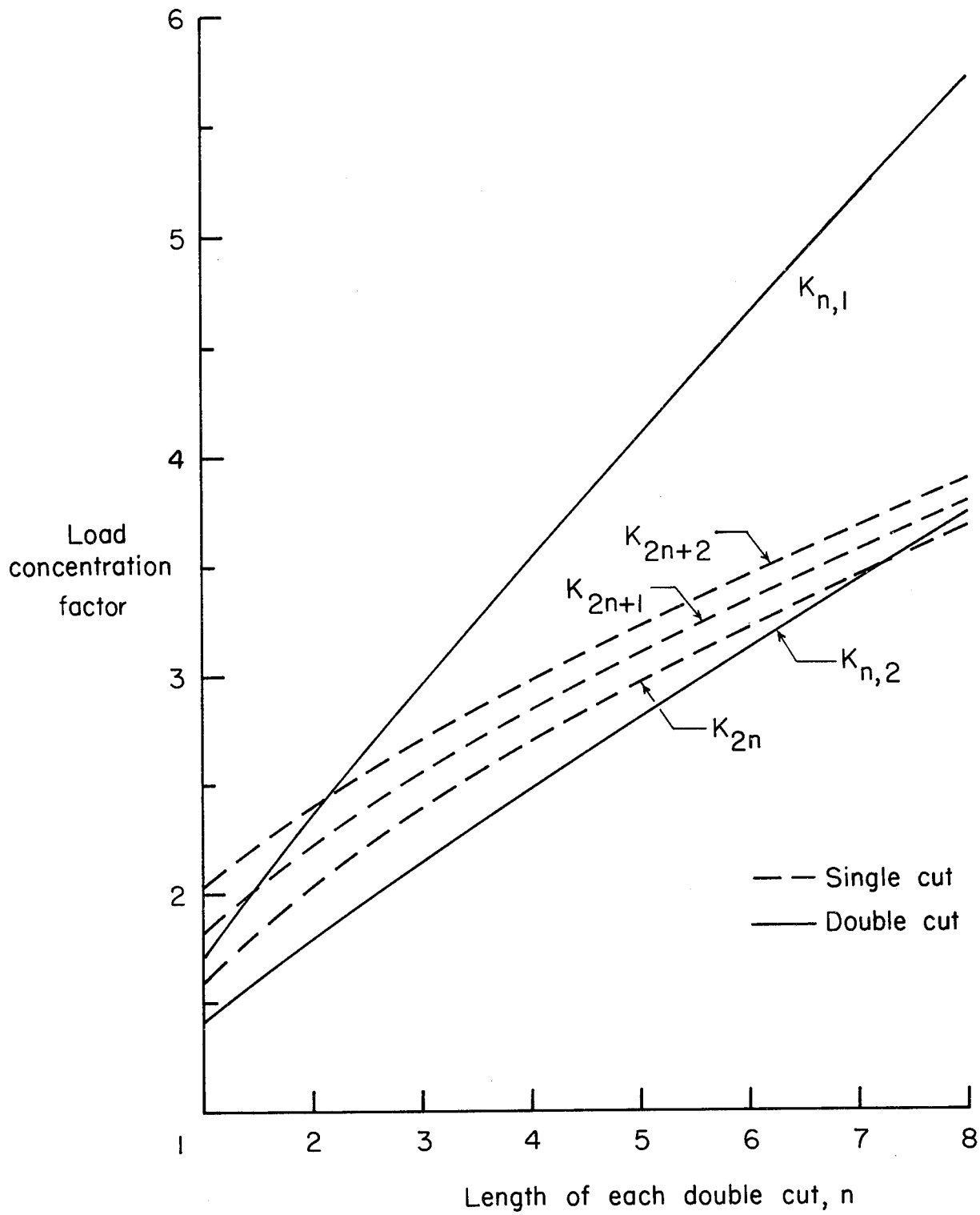


Figure 3.- Comparison of filament load concentration factors for single and double cuts.

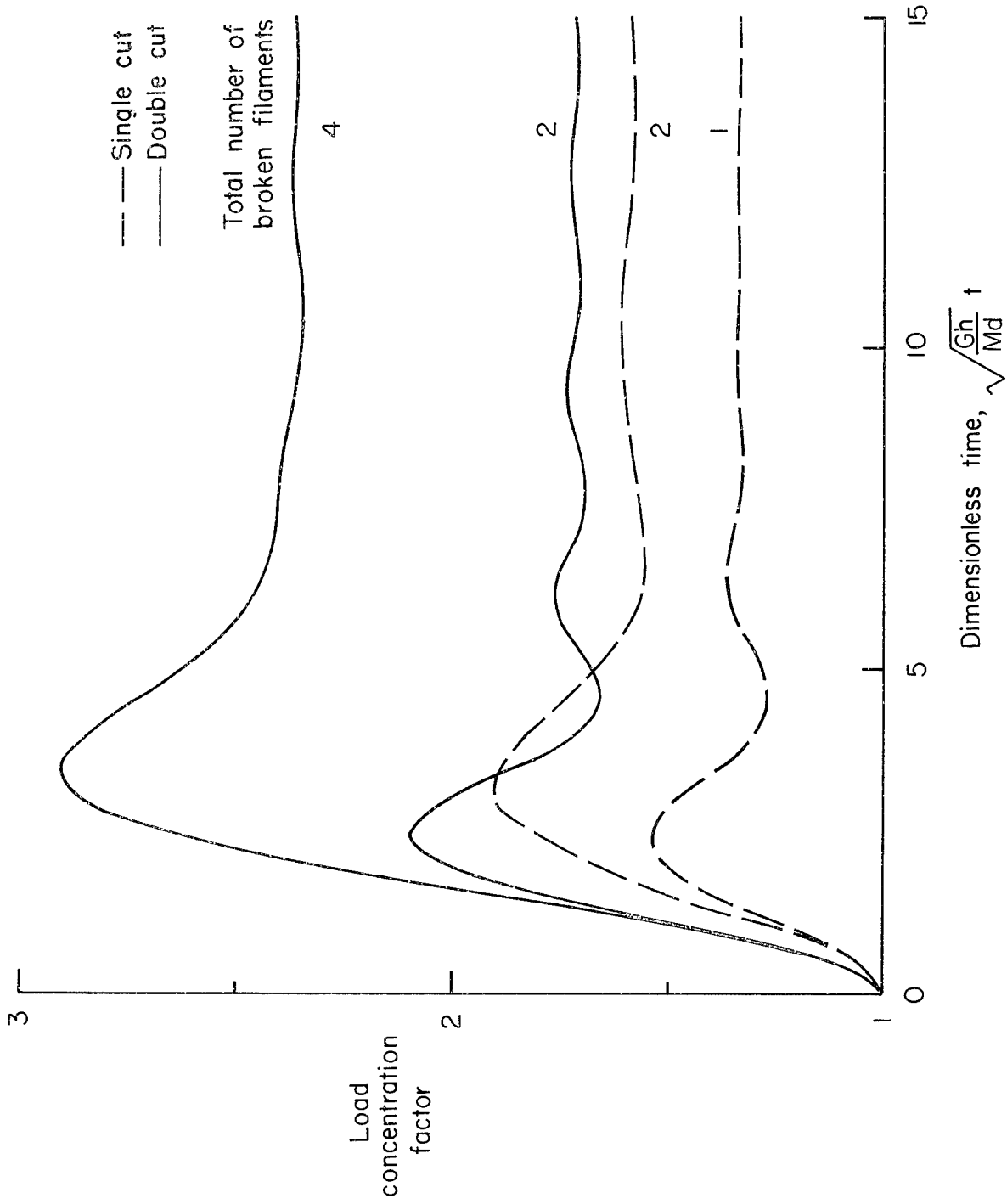


Figure 4.- Dynamic load concentration factors.

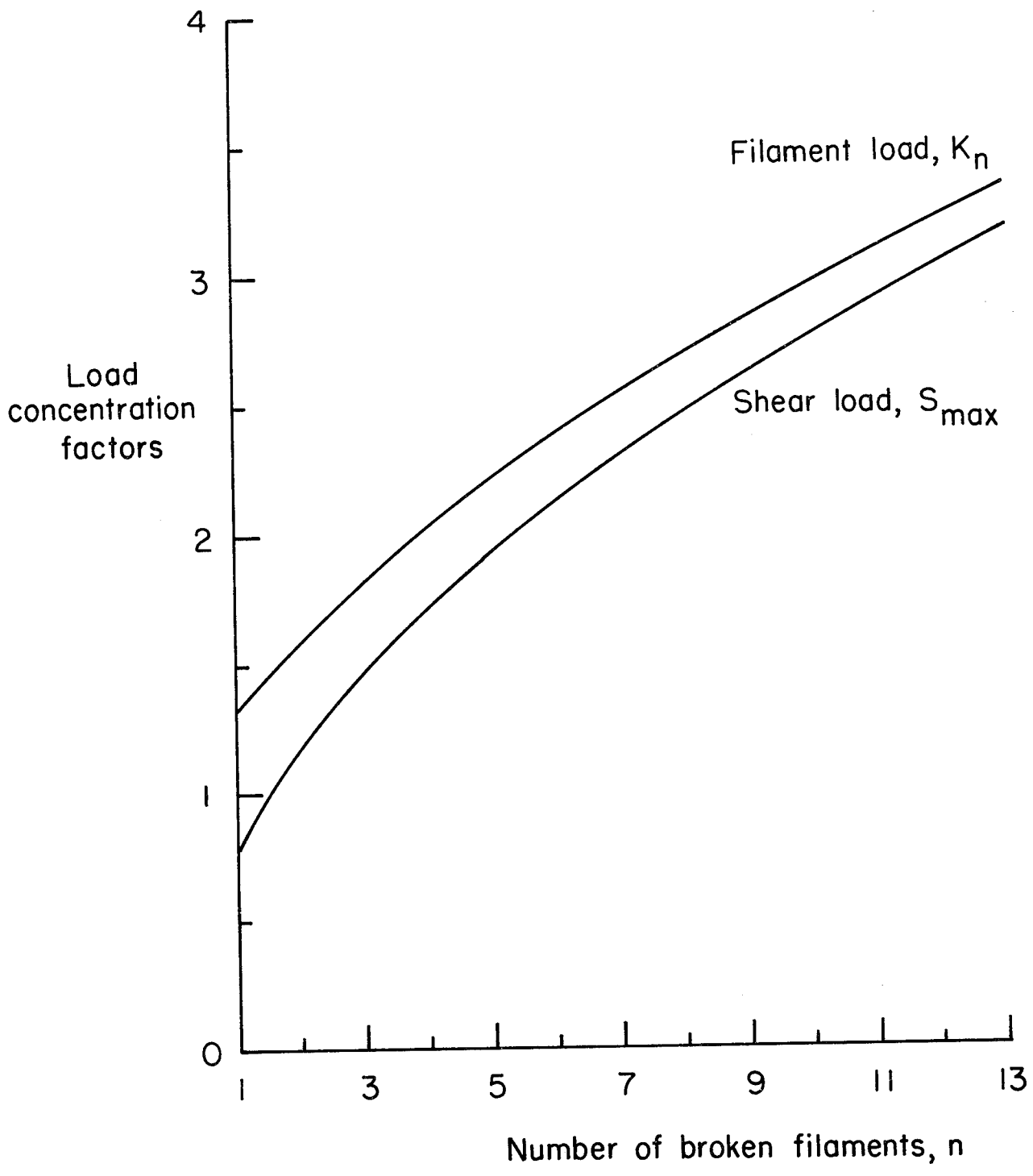


Figure 5.- Single-cut concentration factors for filament load and matrix shear force.

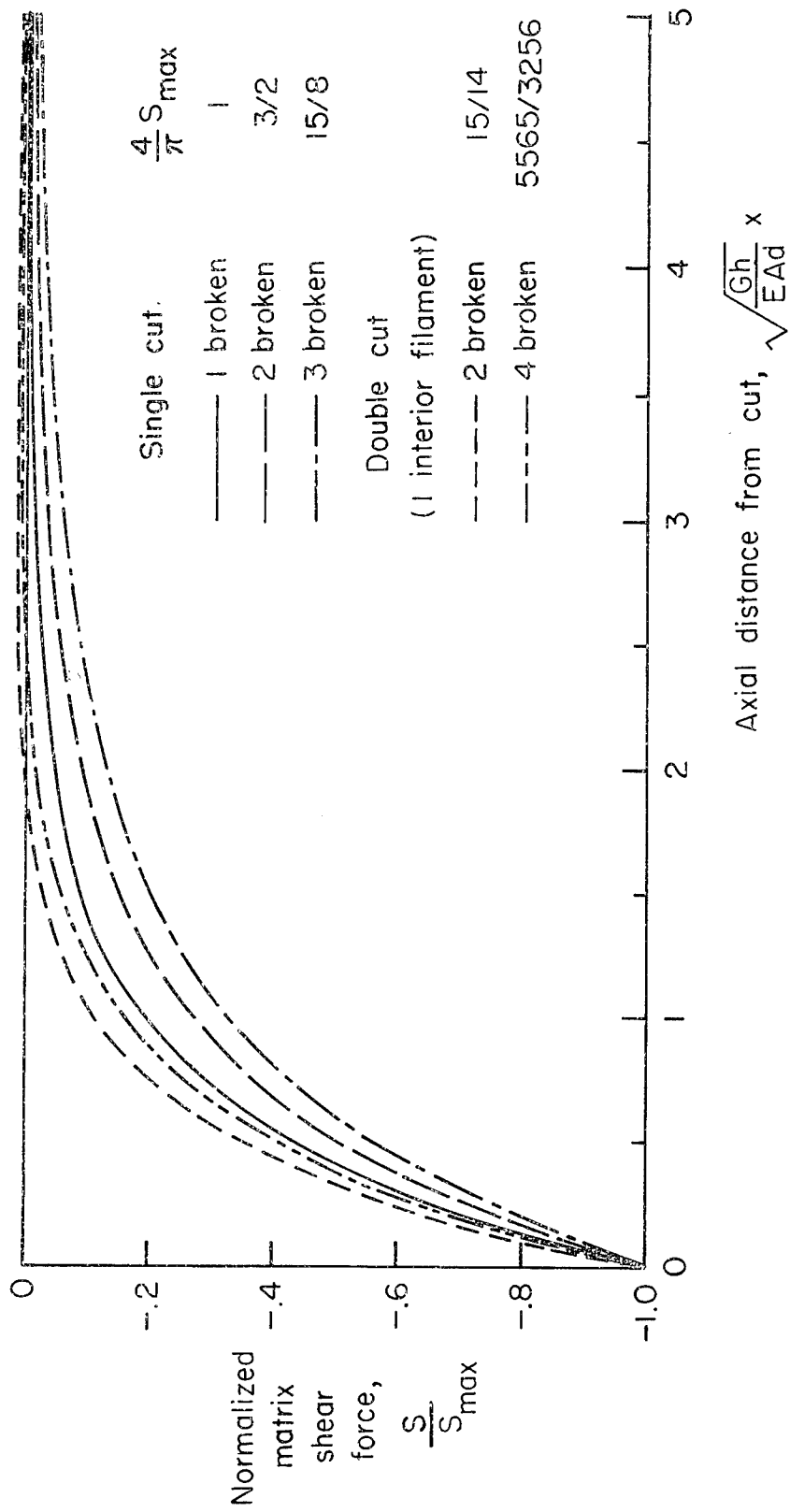


Figure 6.- Variation of most severe matrix shear forces with axial distance from the cut.

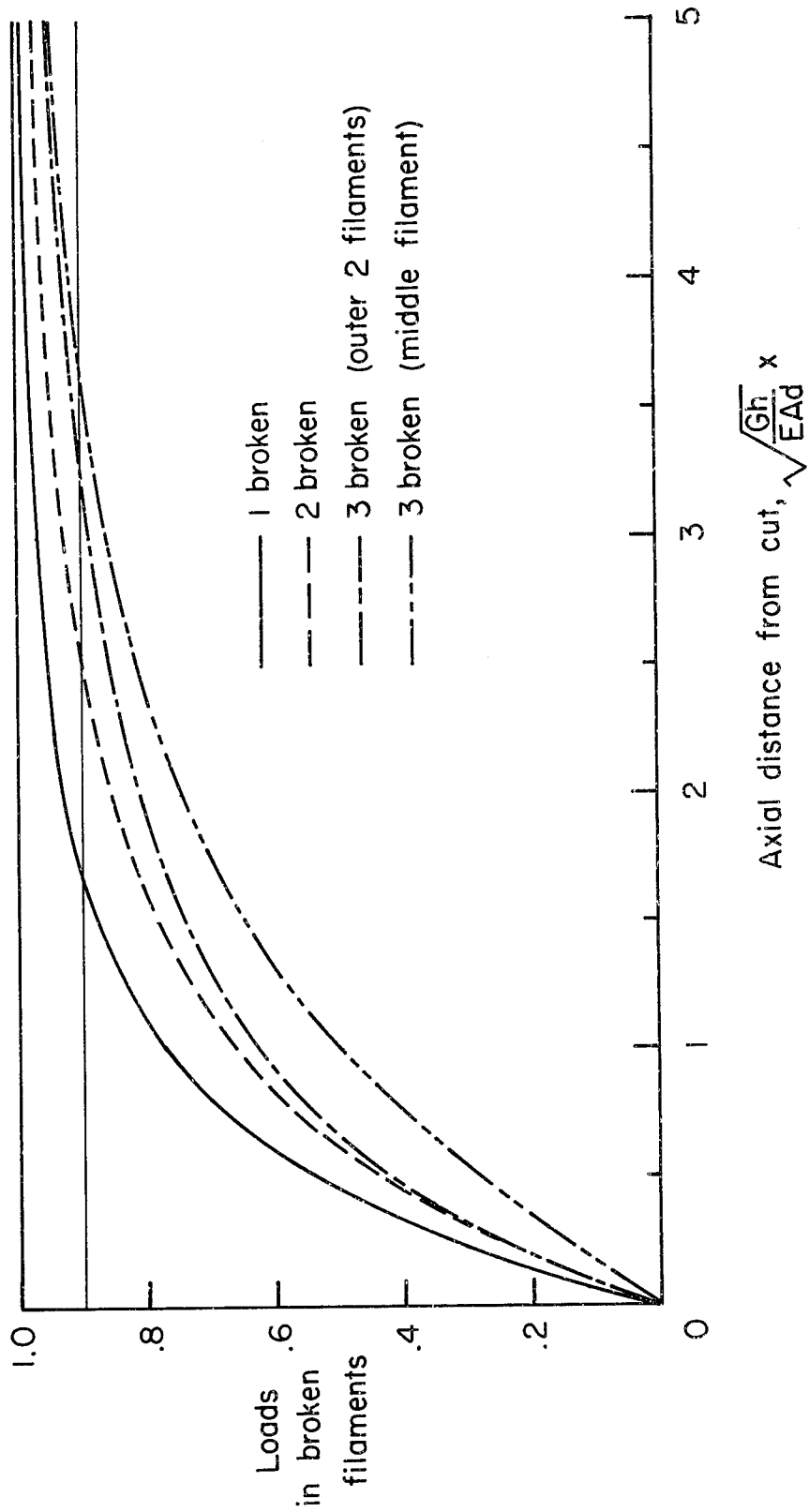


Figure 7.- Loads in broken filaments near a single cut.

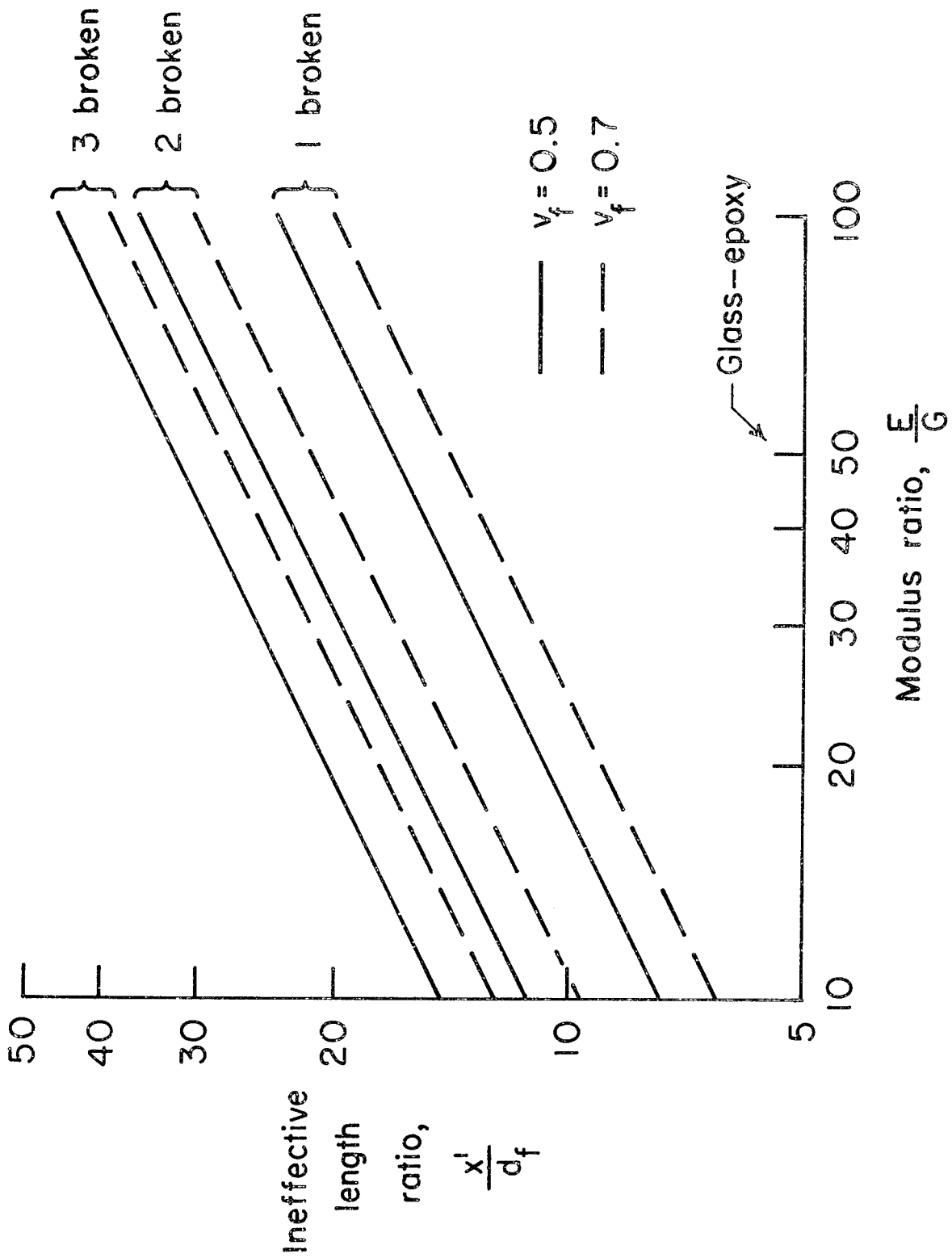


Figure 8.- Ineffective filament length variation with cut length and modulus ratio.